5-1-1984

An investigation into the penumbral dose of a bloxel, (block element) matrix-design block to replace currently utilized radiation treatment field shaping techniques

Theresa Ciccone

Rochester Institute of Technology
Bachelor of Science Degree Thesis

An Investigation into the Penumbral Dose of a Bloxel, (Block Element) Matrix-Design Block to Replace Currently Utilized Radiation Treatment Field Shaping Techniques

by

Theresa Ciccone

April, 1984

Thesis Advisor: Dr. Larry Simpson
University of Rochester Cancer Center

ROCHESTER INSTITUTE OF TECHNOLOGY
Imaging and Photographic Science Department
Rochester, NY

Bachelor of Science Degree Thesis

The Bachelor of Science Degree Thesis of Theresa J. Ciccone has been examined and approved by the thesis committee as satisfactory for the thesis requirements for the thesis requirement for a Bachelor of Science Degree.

Larry Simpson
Dr. Larry Simpson, thesis advisor

Theresa J. Ciccone
Theresa J. Ciccone

Ronald Francis
Dr. Ronald Francis

May 14 1984
Date

Thesis Release Permission Form

ROCHESTER INSTITUTE OF TECHNOLOGY
Imaging and Photographic Science Department

Title of Thesis:

An Investigation into the Penumbral Dose of a Bloxel, (Block Element) Matrix-Design Block to Replace Currently Utilized Radiation Treatment Field Shaping Techniques

I, Theresa Ciccone, prefer to be contacted each time a request for reproduction is made. I can be reached at the following address.

145 Lincoln Street
Revere, MA 02151

Date 5/14/84

ACKNOWLEDGEMENT

The author would like to recognize the assistance of the following:

The Lord from whom all good things come.

Dr. Larry Simpson for all of his time and help extended in advising.

Dr. Jim McFaul for his time and effort in technical aid and spiritual counseling.

The faculty and staff of the Imaging and Photographic Science Department at R.I.T., notably Dr. Francis, Dr. Brower, and Mr. Engeldrum.

The members 1984 graduating class of the Imaging and Photographic Science curriculum for their support and imparticular the honor of their friendship.

DEDICATION

This thesis is dedicated to Teresa DeSantis whose love, kindness, and faith in God has touched me in every area of my life.

For their patience, generosity, and love which has been my strength, John Jr., Nancy, John III, and Eric Ciccone also share in the dedication.

TABLE OF CONTENTS

TABLE OF TABLES

TABLE OF FIGURES

TABLE OF SYMBOLS

Figure 2:

f = Source to receiver distance.
s = Source.
fc = Source to collimator distance.
p = Penumbral spread

Figure 4:

SBD = Source to block distance.
SFD = Source to film distance.
B = Block.
S = Source.

Figure 5:

1 = Scan number one
2 = Scan number two
3 = Scan number three

ABSTRACT

Presented here is an investigation to establish physical rationale for the acceptance by physicians of a new form of blocking device for radiotherapy.

The focus of the investigation is on the percent dosage obtained in the penumbral regions created by 6 mm and 9 mm stepped-edge blocks, relative to a straight edge, when exposed to 1.25 and 18 MeV photons.

INTRODUCTION

Due to the sensitivity of healthy tissue to radiation, the healthy bone and soft tissue of a cancer patient receiving radiation treatments, is physically blocked while in the field of propagation. The risks to healthy tissue from a given dose of radiation are higher among children than adults due to an increased sensitivity in persons of younger years. Since there are approximately 10E+9 cells in a cubic millimeter of tissue, to minimize radiation exposure damage, great care is taken not only in the blocking mechanism but also in the positioning of the patient for each treatment session.

The ability to accurately position a patient for each treatment is very important. This becomes particularly vital when therapy is prescribed for cancerous areas adjacent to critical, healthy tissue. However, given that a patient is never in exactly the same spot for each treatment, along with movement by the patient during treatments, perfectly accurate positioning of the block is difficult. Consequently, there is an uncertainty associated with the spatial distribution of the absorbed dose in the penumbra (edge). The probability associated with its location is assumed to be described by a gaussian distribution.

Several options regarding blocks have been explored and used in radiation oncology practice. One type of block is made of lead glass [1,2]. However, these are fragile and difficult to make for each patient. Durability may be attained with the use of shields made of lead acrylic [1,2,3]. Lead acrylic blocks are also hard to make; yet they reduce surface dose of an unblocked Co60 source by 20 - 25 percent [1]. Opaque filters have the disadvantage of interfering with light localization of the treatment field [1]. Bailey and his associates investigated the use of shields molded from lead sheets lined with a thin layer of wax and determined this effective for the treatment of superficial lesions [4]. What is desired is a total block mechanism.

Currently the overwhelming system used in radiotherapy clinics is a block made of a low melting point lead alloy [5-10] which has a transmission rate of 1.5 - 3 percent [2].

The production of these lead blocks personalized for each patient, involves several steps. Initially the radiotherapist must map out the desired dimensions of the blocked regions on an x-ray simulator film. Styrofoam is then cut with a hot wire device to form the mold in which the molton alloy is then cast. Once the block has cooled it may then be inspected for voids or defects and repaired accordingly [7,8]. The thickness of the block is determined by the intensity of the source to be used. Increasing intensities require thicker blocks, however consideration

must be given to the weight of the resultant block.

A few of the drawbacks to this method of construction are time, health hazards to the machinists, and cost. The time involved from design to treatment setup is about two days. Once the treatments have begun, if a repair or modification must be done to the block, as dictated by the radiation oncologist or medical physicist, therapy may be interrupted for up to three days. This is the critical drawback which encourages this investigation into a new blocking technique and its physical rationale.

The construction technicians may periodically be given lab tests to monitor their toxicity levels, because of the alloys used. Safeguards must be taken against the constant danger of inhalation of metallic dust or vapors, ingestion, skin absorption of the alloy, etc. [7].

Another problem with this current system is the cost. The price of materials, equipment, and labor must be figured into the costly expense of radiation treatments.

The ideal consequence of any shielding technique employed, is to provide 100 percent irradiated dosage within the tumor boundries while eliminating exposure to the normal tissue. However, [figure 1] a plot of dosage vs. field distance illustrates that this is not the result [12,15].

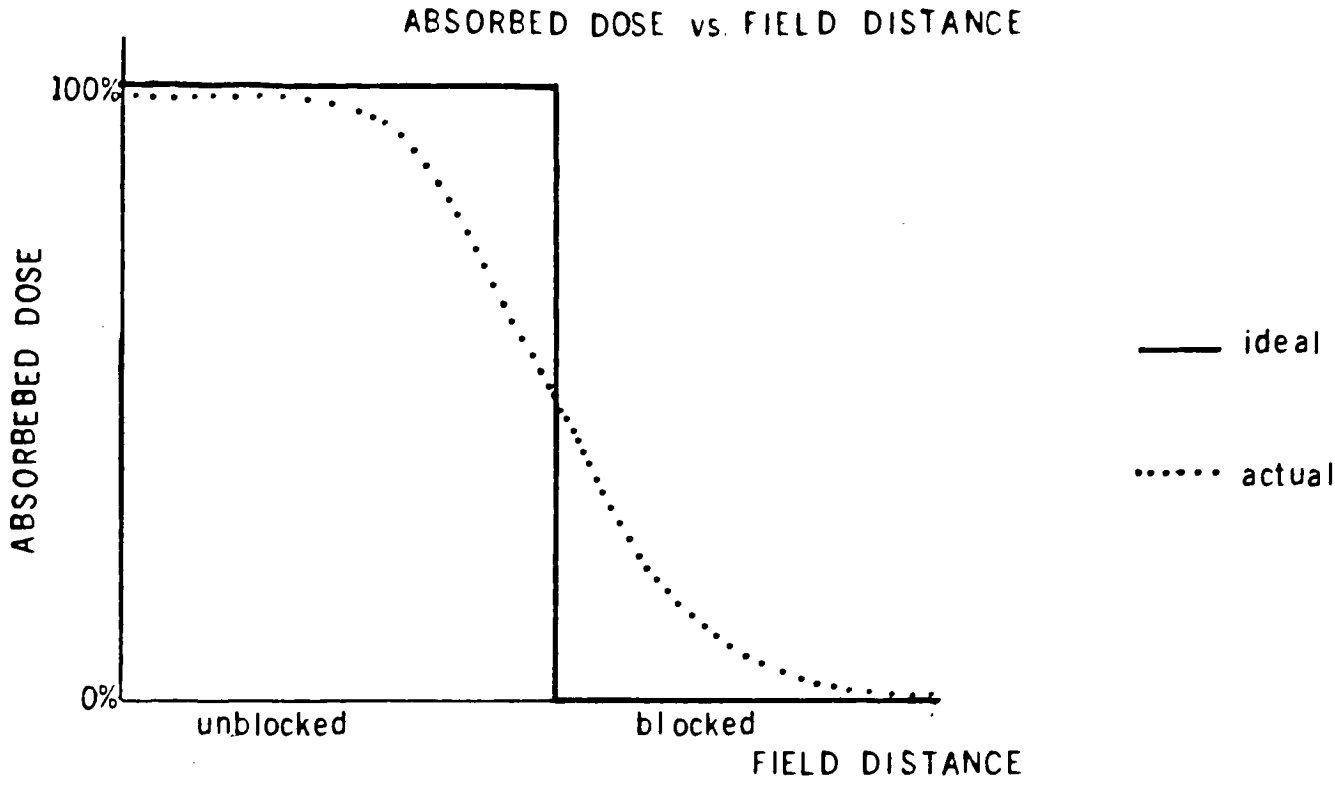

Fig.1

This physical phenomenon known as a penumbra has a width defined by the distance between the 90 percent and 10 percent isodose lines [5,13] and is always experimentally measured. The penumbra can be thought of as the edge response function.

Some of the factors influencing the penumbra are the source diameter, the distance from the source to the end of the block, the distance from the block to the shielded tissue of interest in the patient, and the thickness of the overlying tissue in the blocked regions [14,15]. Johns and Cunningham [15] illustrate a penumbra due to the collimator as shown in figure 2.

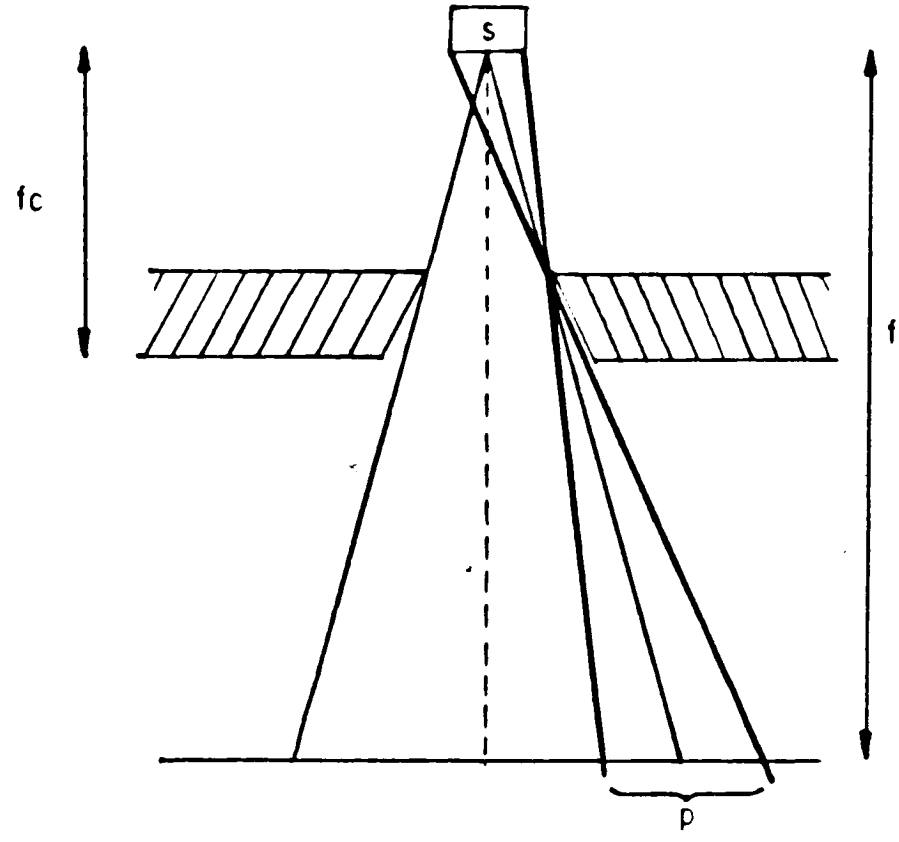

GEOMETRIC PENUMBRA (15)

Fig.2

The geometric penumbra width may be quantified by the equation :

$$P = S \times (F - FC) / FC$$

where S is the source diameter, FC is the distance from the source to the collimator, and F is the distance from the source to the receiver [15].

This is an investigation into the spatial distribution of the absorbed penumbral dose obtained with utilization of lead alloy shields; simulating a bloxel (block element) matrix system. This study will assist in establishing the rationale for an automated bloxel design for the future (See figure 3).

BLOCKING FORMS

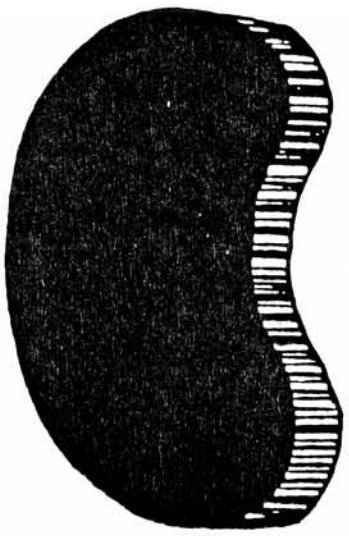

CONTINUOUS

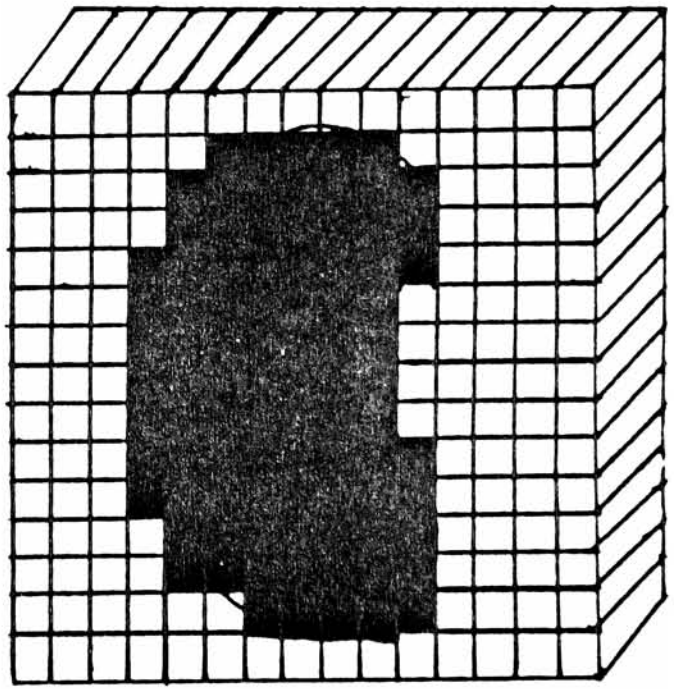

BLOXEL MATRIX

Fig.3

If the continuous edge can be thought of as a stepped edge with step dimensions of zero, then this study may be termed one of establishing maximum radiologically-acceptable bloxel size.

The purpose of this investigation is to lay the groundwork for a digitally-controlled bloxel system which could provide the physician with dynamic control over personally-designed blocks for each cancer patient. Firmware could be designed and provided in the future to allow the physician to digitally manipulate desired block dimensions in real time, and hence immediately provide the best group bloxel fit. This could then be stored in memory making it easily accessible for the patient's subsequent radiotherapy sessions. This system would be universally applicable to all patients, as reproducible as the currently established blocking techniques, and would be cost effective. Further investigation into it's design, prototype manufacture, and testing can be initiated only after these preliminary studies are completed.

STATEMENT OF WORK

1. Block Design and Fabrication

1.1 The bloxel, (block element) block models were cast by machinists at the University of Rochester Cancer Center into styrofoam molds, which were cut by a hot wire device.

1.1.1 The blocks are composed of a lead alloy, Lipowitz metal:

13.3 % tin

50.0 % bismuth

26.7 % lead

10.0 % cadmium

with a density of 9.4 g/cm-cubed at 20°C. [7]

1.1.2 The stepped edge sizes are 3, 6, 9, 12, and 15 mm in image size at 100 cm from the source. The blocks are 10 cm thick and have a transmission rate of:

0.5 % - 0.6 % for a Co-60 source,

and

2 - 3 % for an 18 MV source. [7]

2. Film Type and Specifications

2.1 Kodak XV2 Rapid Process film was used because of its current use at the University of Rochester Cancer Center for film dosimetry.

2.2 Development was initially to be done on a JOBO temperature-controlled processor purchased by the University of Rochester Cancer Center. Modifications were made to permit processing to both the inner and outer emulsion layers. When the process was determined to be under control the processor broke down. Time constraints necessitated the use of the Cancer Center's X-Omat

2.3 Sensitometric strips were used to test the reproducibility of the University of Rochester Cancer Center's X-Omat. The results between samples, for a particular step, were found to be within 0.04 density units for a given day.

2.3.1 Development was done with a Kodak GBX developer at 95° F for 55 seconds in a Kodak RP X-Omat processor. Fixing was done with Kodak GBX fix.

3. Film Irradiation and Calibration (See figure 4)

3.1 Calibration curves (or H&D curves), were constructed from exposures to 1.25 and 18 MeV photons. The calibration curves enable dose to be matched to corresponding densities subsequently obtained on film. The exposure rate of the sources are calibrated with ion chamber standards which give the absorbed dose rate; traceable to the National Bureau of Standards.

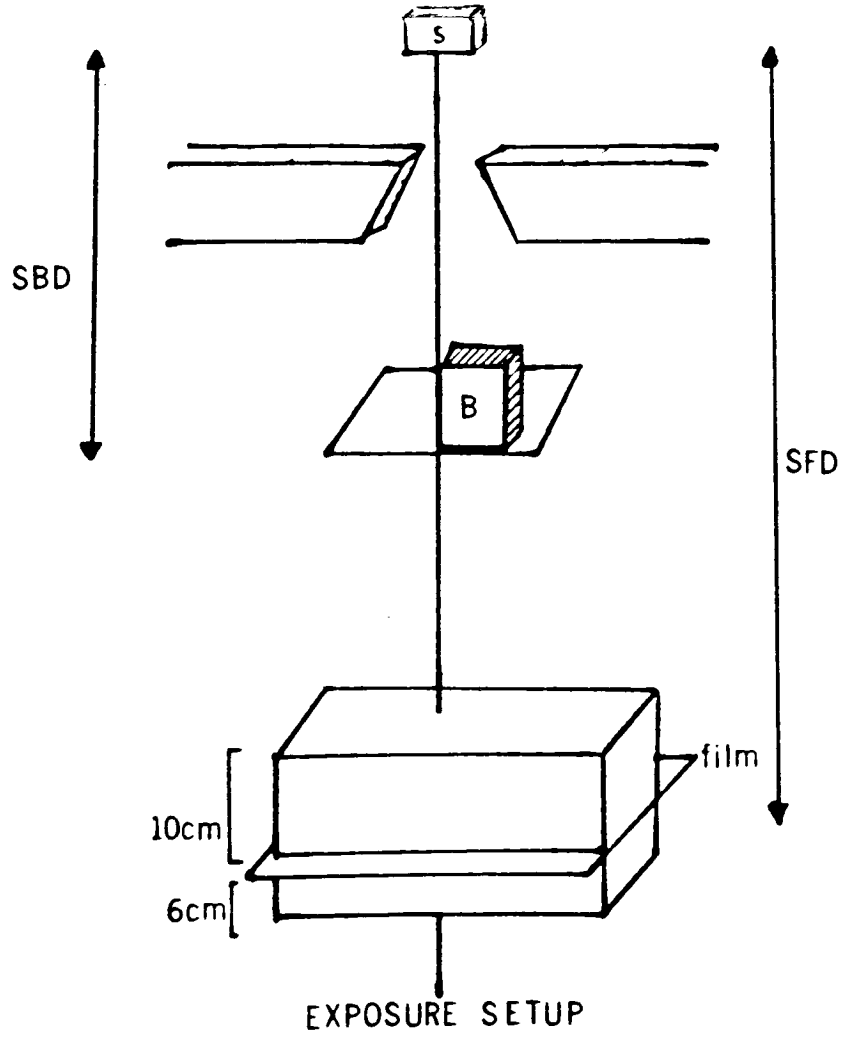

Fig.4

3.1.1 All exposed film samples were developed on a particular day to avoid day to day variations in the X-Omat processing. However, the calibration film samples and the block edge exposure sample were not processed on the same day. To account for day to day variations exposures were made on the straight line portion of calibration curves and the deviation used as a multiplicative factor.

3.1.2 Exposure energies of 1.25 and 18 Mev were chosen due to their prevalent use in radiotherapy.

3.1.2.1 Picker Corp. CB-80, a Co-60 source with 1.17 and 1.33 Mev monoenergetic photons (1.25 MeV mean energy) where:

source diameter = 2 cm.,

and source to film distance = 124.5 cm.

3.1.2.2 Therac-20, a medical electron linear accelerator with an 18 MV bremsstrahlung spectrum (mean energy, 7.6 MeV) where:

source diameter = 0.3 cm.,

and source to film distance = 124.5 cm.

4. Block Exposures

4.1 Exposures made with both the stepped edge blocks and the straight edge block were made with each of the previously mentioned sources (See section 3). A depth of 10

cm. in water equivalent plastic was chosen to simulate clinical-patient condition. This depth represents the average dosage depth in a patient.

4.1.1 Co-60 source:

source diameter = 2 cm.,
source to block distance = 64.5 cm.,
source to film distance = 100 cm.

Water equivalent plastic:

10 cm. on top of the film,
6 cm. beneath the film.

Radiation field size:

10 x 10 cm.

4.1.2 18 MeV source:

source diameter = 0.3 cm.,
source to block distance = 64.5 cm.,
source to film distance = 100 cm.

Water equivalent plastic:

10 cm. on top of the film,
6 cm. beneath the film.

Radiation field size:

10 x 10 cm.

5. Densitometry

5.1 Edge scans were made of each of the film samples on an Ansco Model-4 Microdensitometer.

5.1.1 The straight edge exposures were scanned perpendicular to the edge.

5.1.2 To examine the effect of a discontinuous edge relative to a straight edge, microdensitometer scans were made perpendicular to a theoretical straight edge for the 6 mm. and 9 mm. (image size) block models.

5.1.2.1 Three types of scans were made on the bloxel model blocks.

Scan types:

1 - Scans made through the the "peak" that was placed on the central axis; extending through the open field edge.

2 - Scans made through the point half way between the peak and the trough.

3 - Scans made through the trough of a period.

A reference line was drawn on each film sample parallel to the imaginary straight line adjoining the peaks of the cycle, to enable the spatial matching of the various scan types. See figure 5.

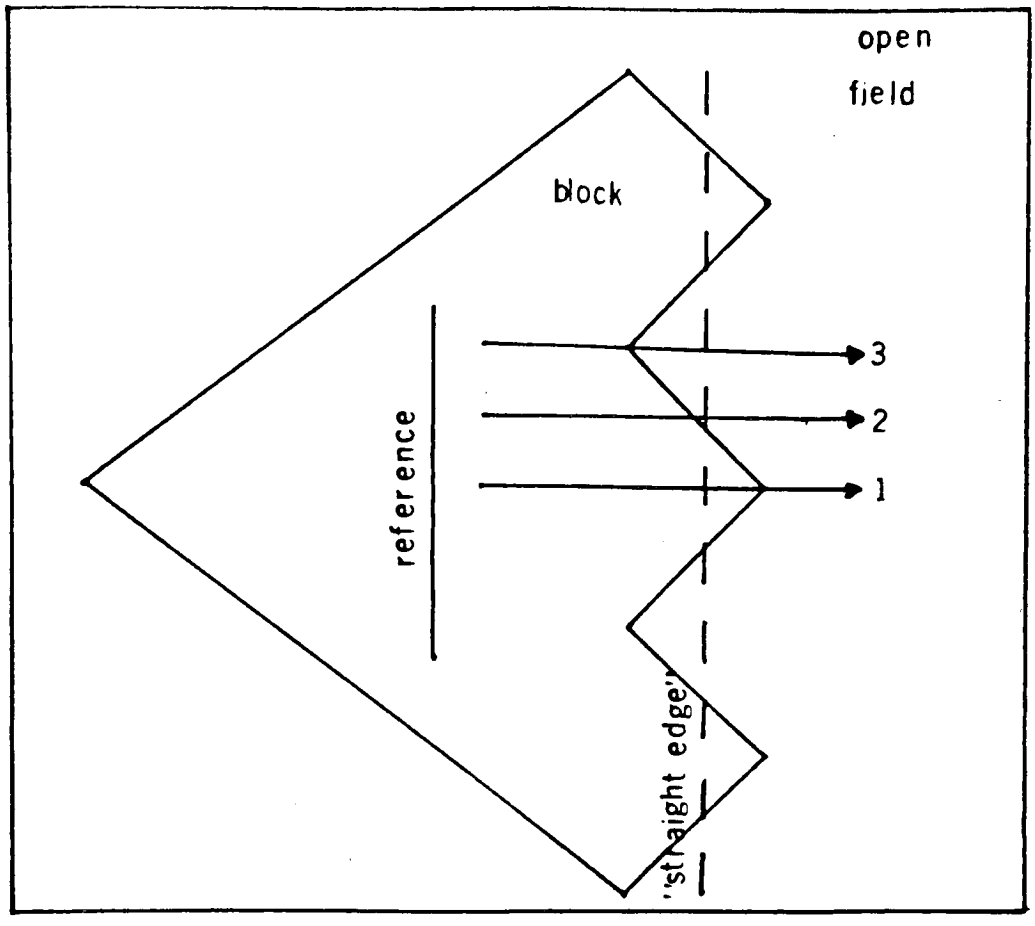

MICRODENSITOMETRY SCAN TYPES

Fig.5

6. Penumbral Dose Evaluation

6.1 The density curves obtained from each of the microdensitometer scans were used to relate net density (density minus base plus fog), to percent absorbed dosage, by means of a calibration curve. (Section 3)

6.1.1 The percent absorbed dose data is shown with the bloxel model data relative to the same data acquired with the straight edge block.

RESULTS

Figures 6 & 7:

Calibration curves for the Co-60 and 18 MeV sources respectively. The curves relate Net Density (Density obtained on film - base plus fog of 0.15) to Absorbed Dose (in rads).

Figures 11,12,15,&16:

Percent Dosage is shown relative to distance along the film. This is done each of the two sources for the 6mm and 9mm block sizes. The curves shown represent each of the three scan types (see figure 5), relative the the straight edge scan of the same source.

Figures 9,10,13,&14:

Percent Dosage is shown relative to Distance along the film. This is done for each source and the averaged 6mm and 9mm block sizes.

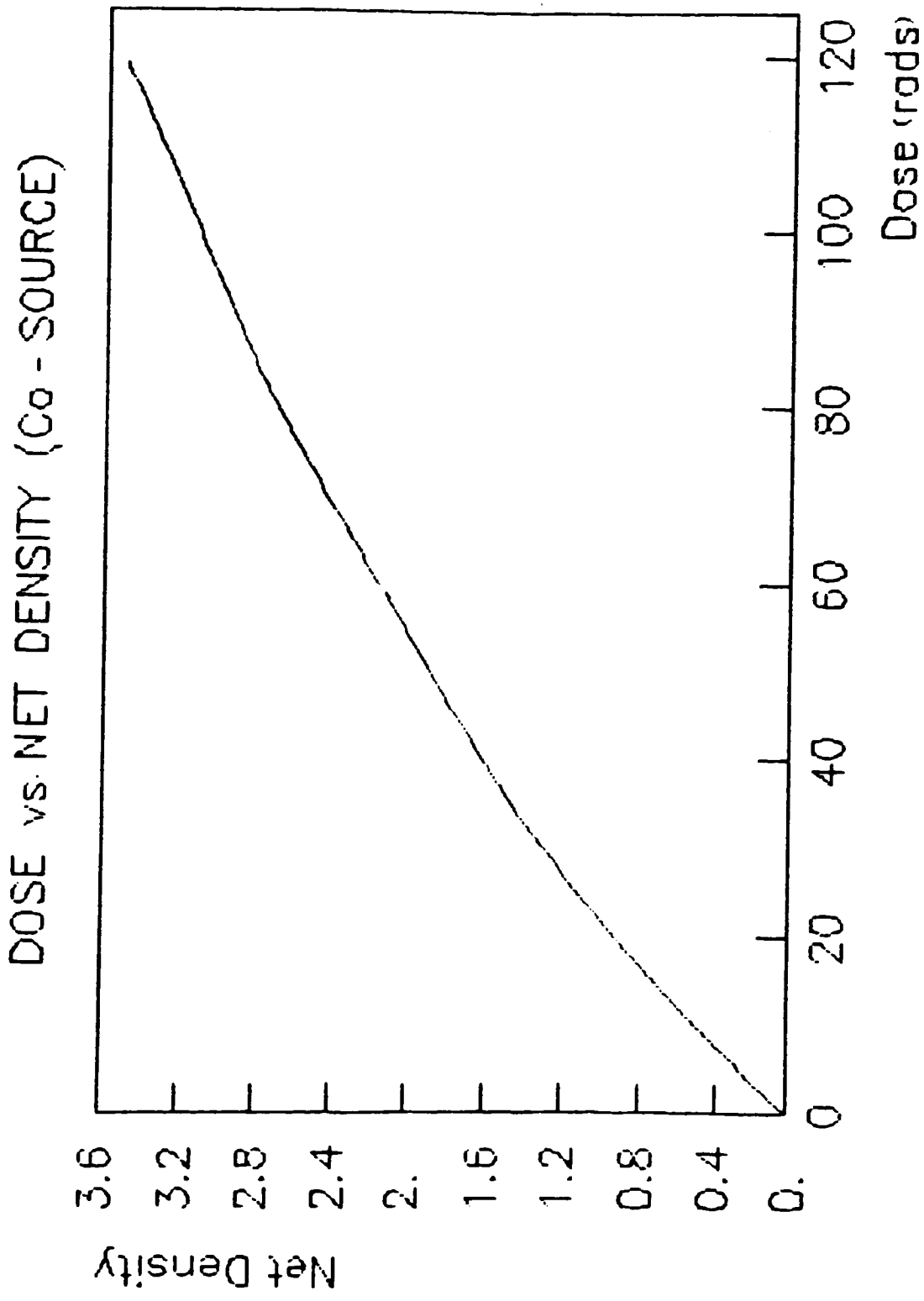
DOSE vs NET DENSITY (Co - SOURCE)
Net Density
3.6
3.2
2.8
2.4
2.
1.6
1.2
0.8
0.4
0.
0
20
40
60
80
100
120
Dose (rads)

Fig.6

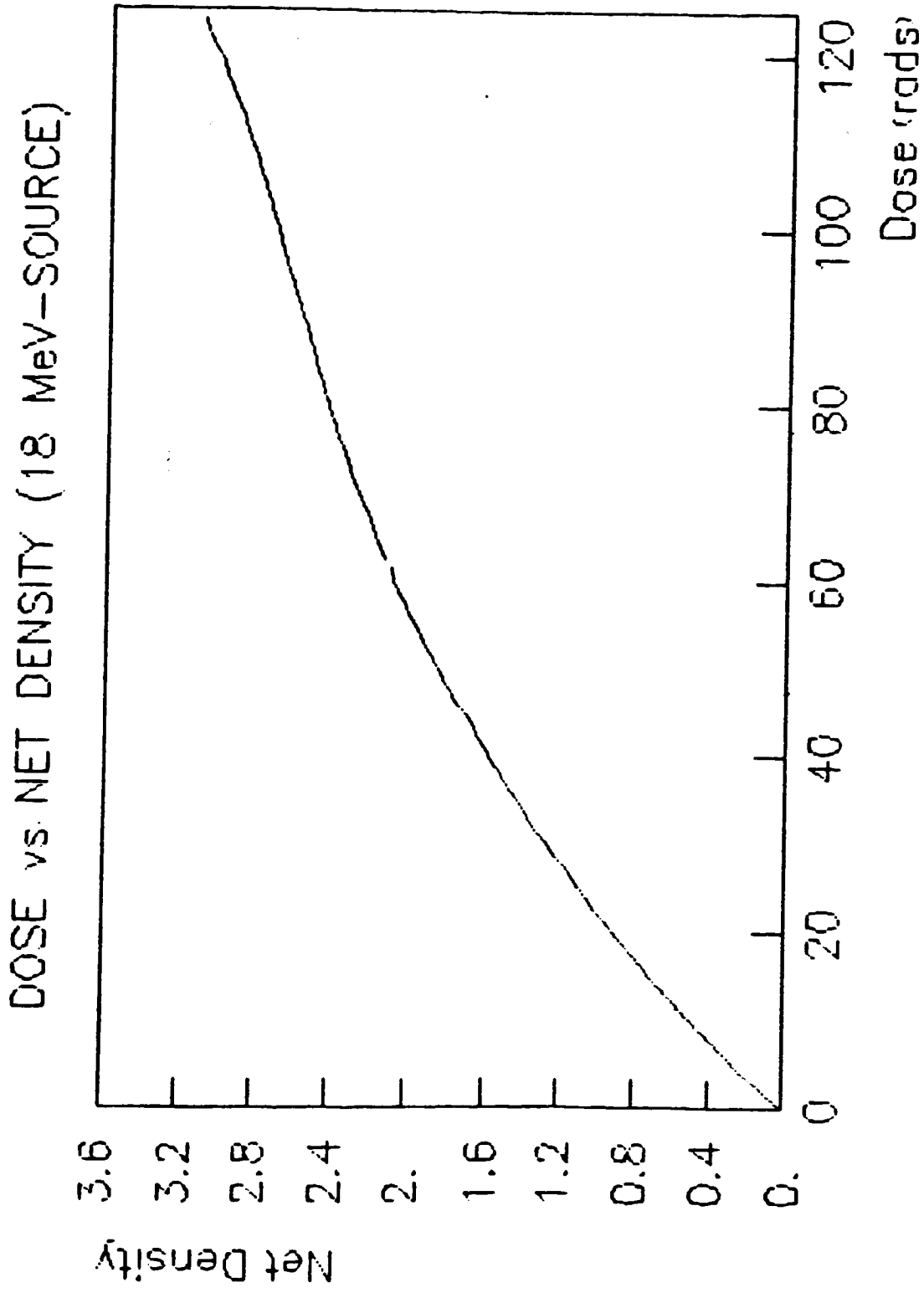
DOSE vs NET DENSITY (18 MeV-SOURCE)
Net Density
3.6
3.2
2.8
2.4
2.
1.6
1.2
0.8
0.4
0.
0
20
40
60
80
100
120
Dose (rads)

Fig.7

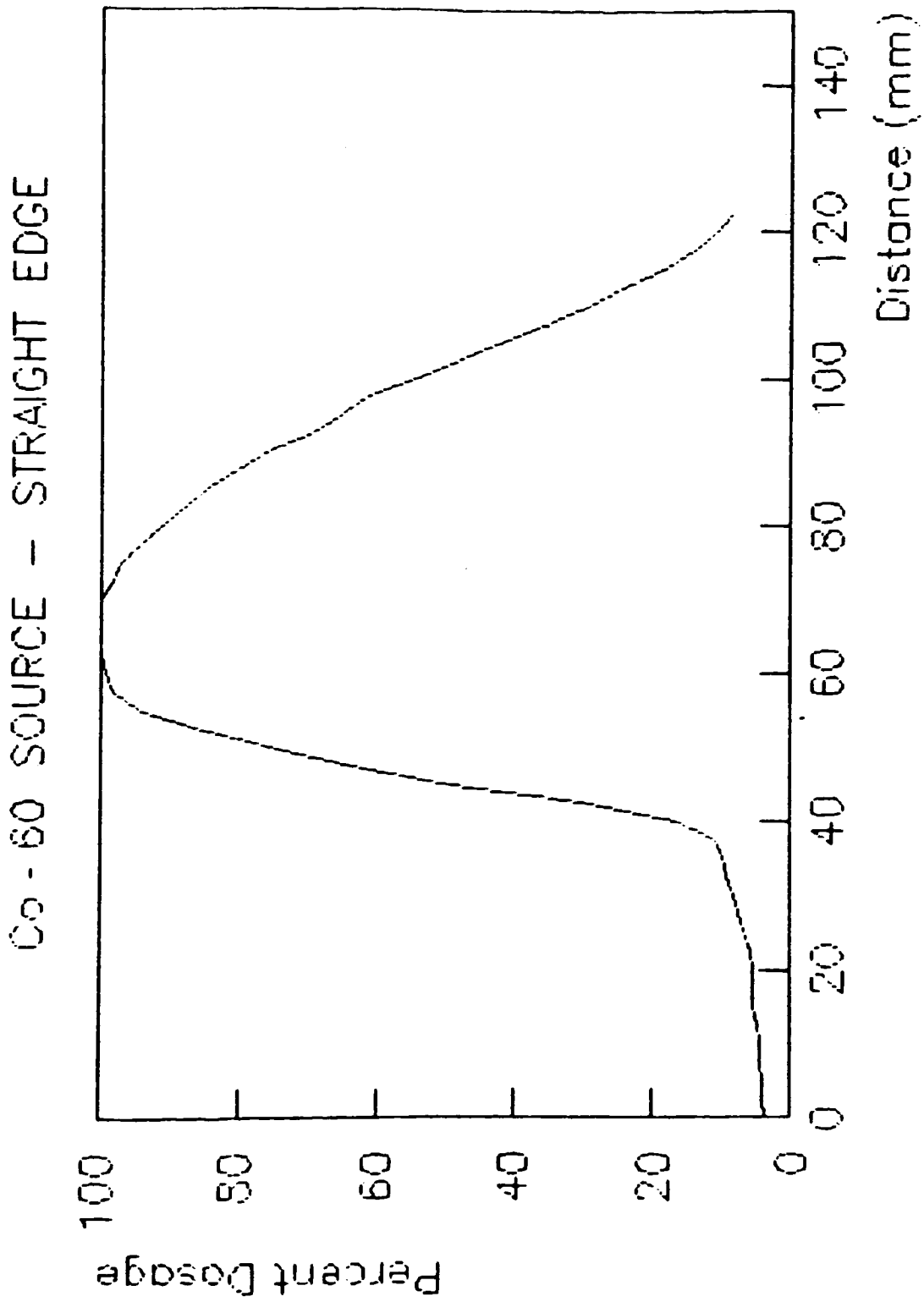
Co - 60 SOURCE - STRAIGHT EDGE
Percent Dosage
100
80
60
40
20
0
0
20
40
60
80
100
120
140
Distance (mm)
STRAIGHT EDGE

Fig.8

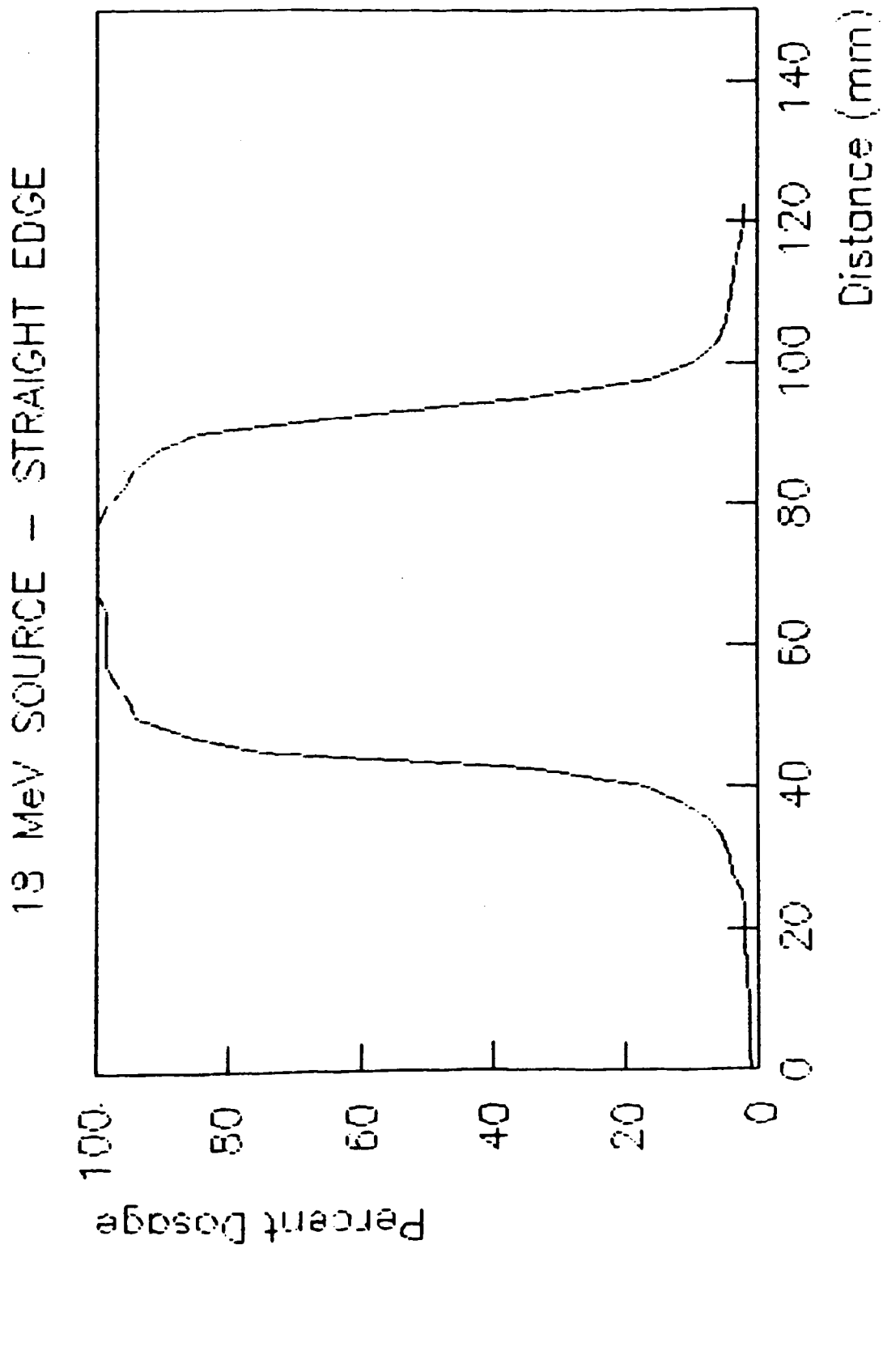
19 MeV SOURCE - STRAIGHT EDGE
Percent Dosage
100
80
60
40
20
0
0
20
40
60
80
100
120
140
Distance (mm)
STRAIGHT EDGE

Fig.9

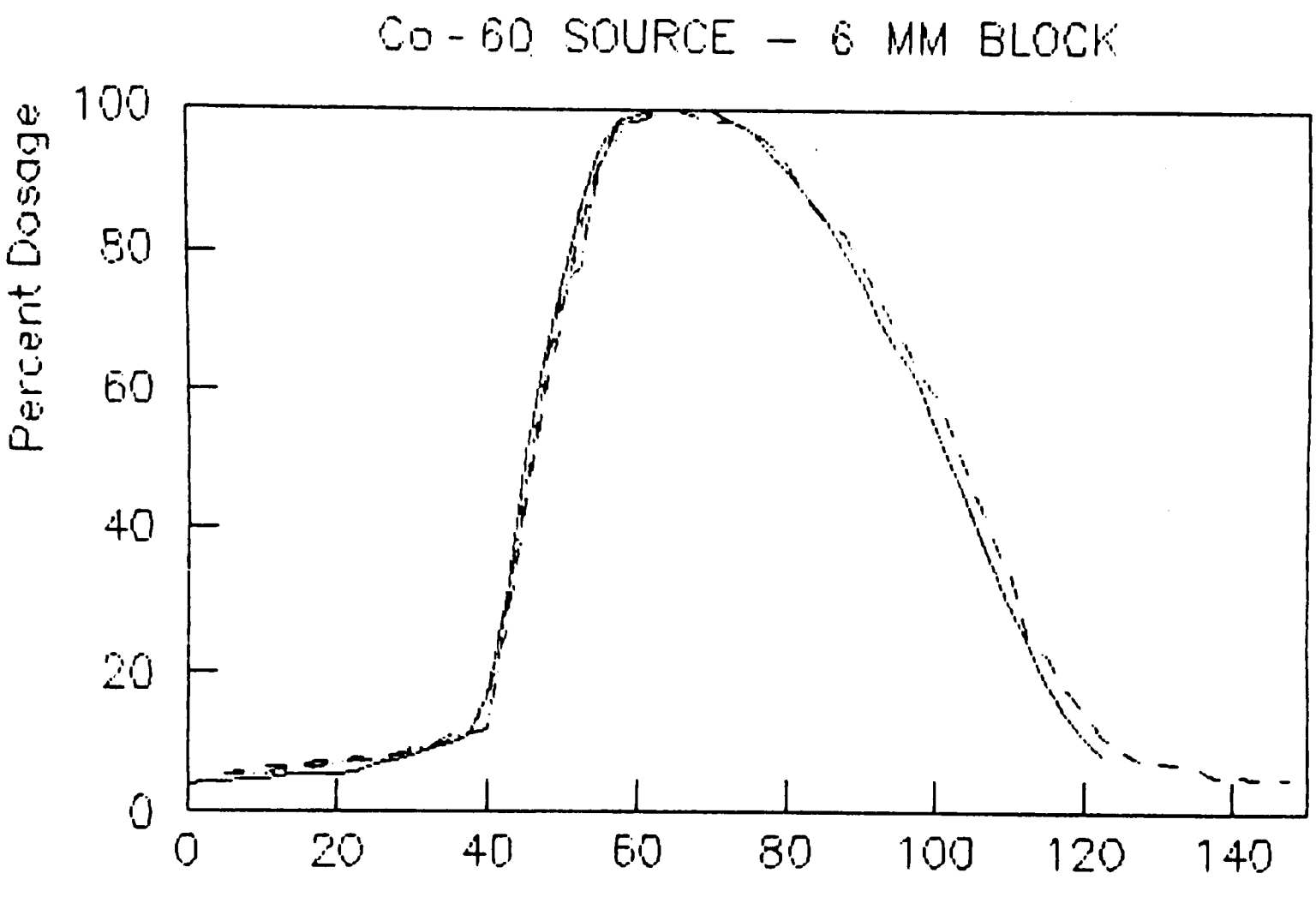

STRAIGHT EDGE
SCAN TYPE #1
SCAN TYPE #2
SCAN TYPE #3

Fig.10

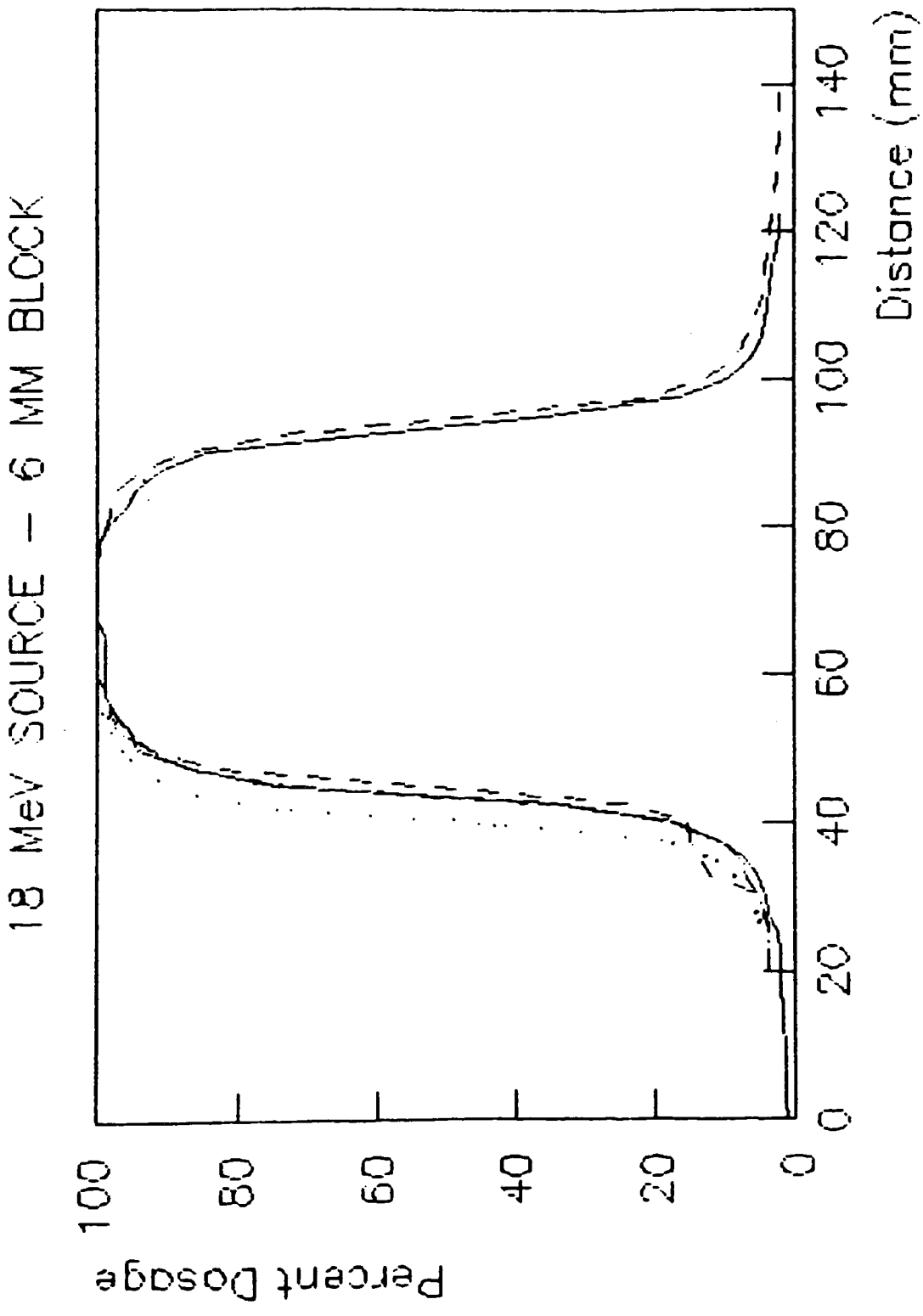
18 MeV SOURCE - 6 MM BLOCK
Percent Dosage
100
80
60
40
20
0
0
20
40
60
80
100
120
140
Distance (mm)
STRAIGHT EDGE
SCAN TYPE #1
SCAN TYPE #2
SCAN TYPE #3

Fig.11

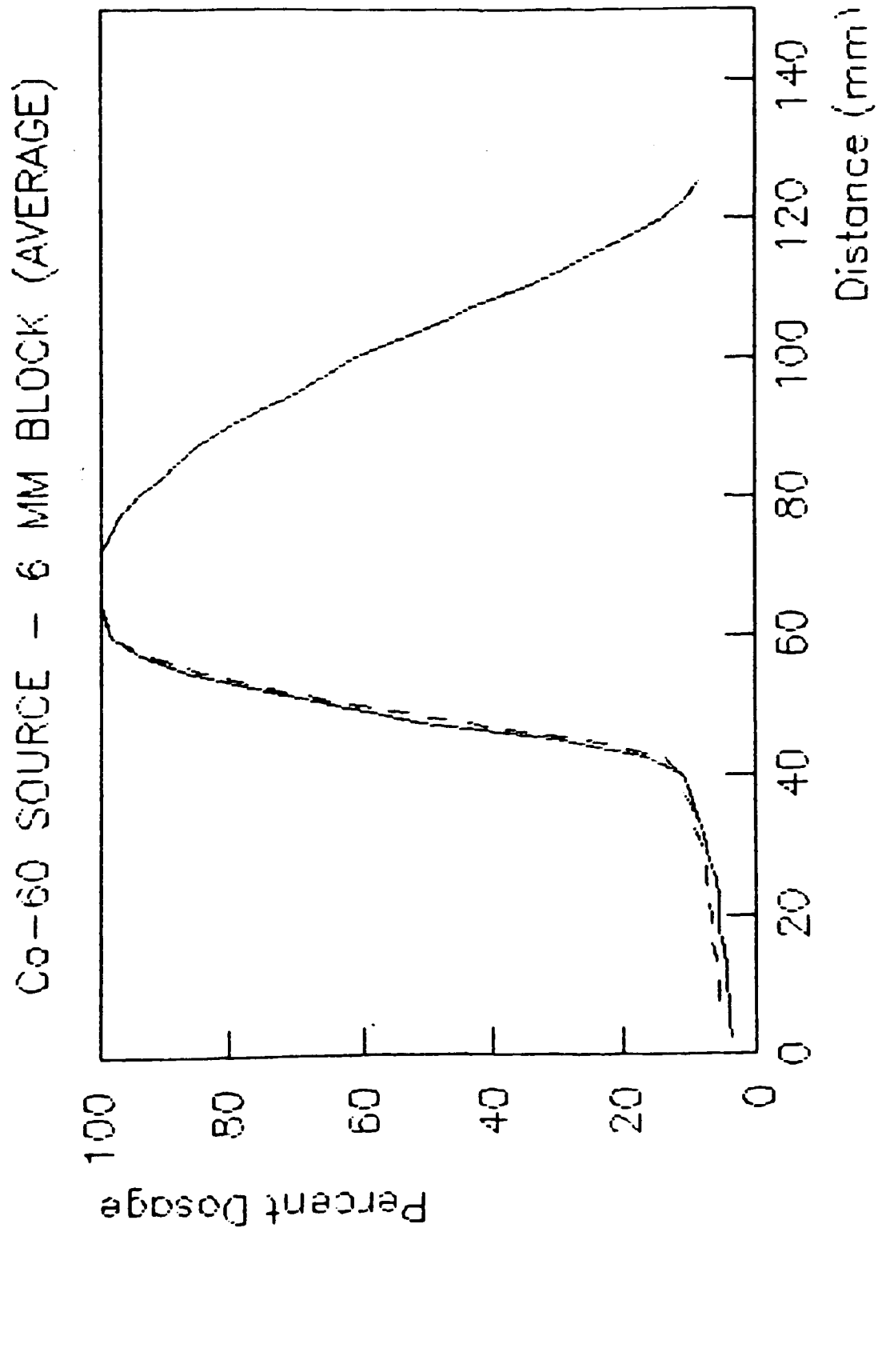
Co-60 SOURCE - 6 MM BLOCK (AVERAGE)
Percent Dosage
100
80
60
40
20
0
0
20
40
60
80
100
120
140
Distance (mm)
STRAIGHT EDGE

Fig.12

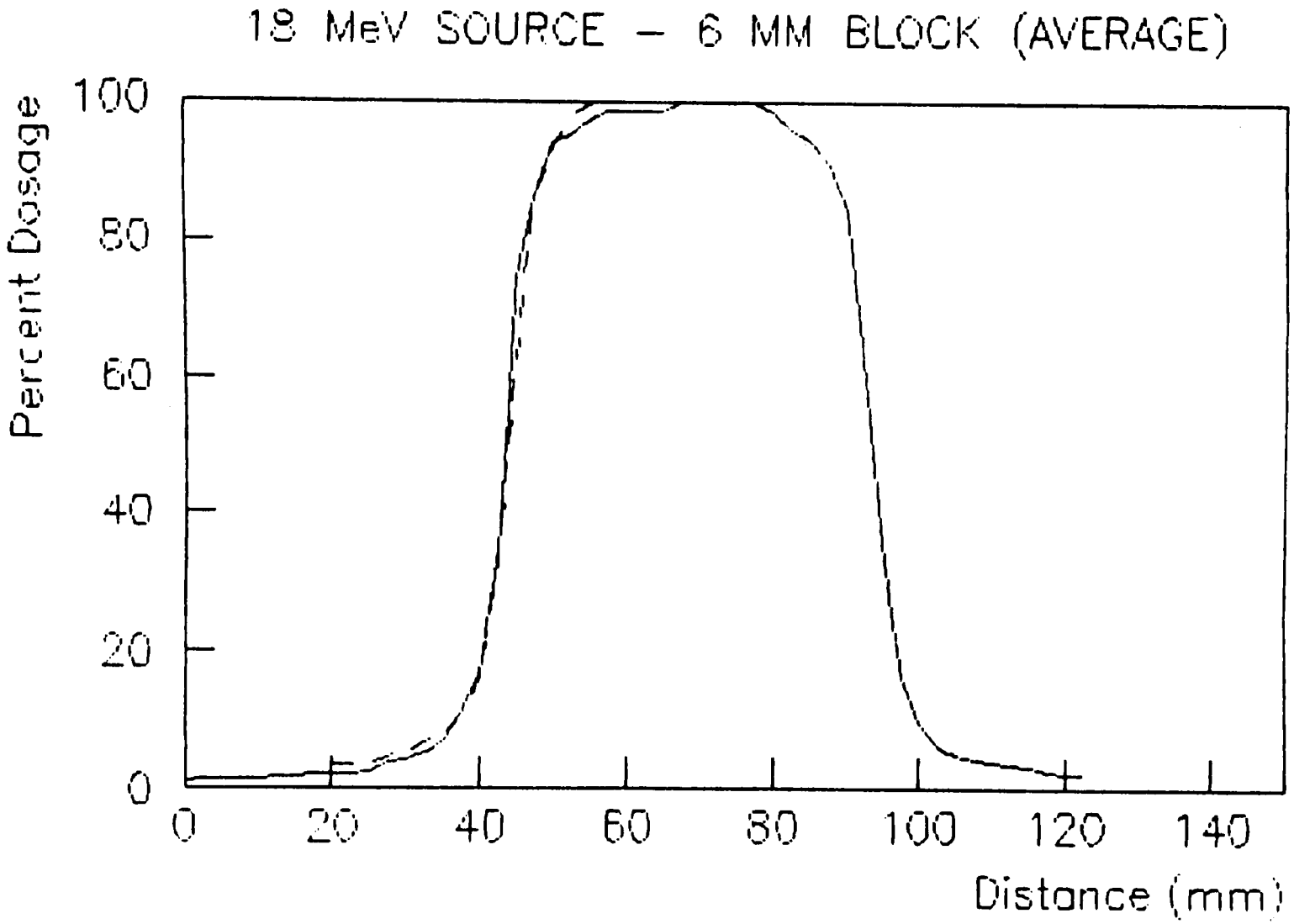

STRAIGHT EDGE

Fig.13

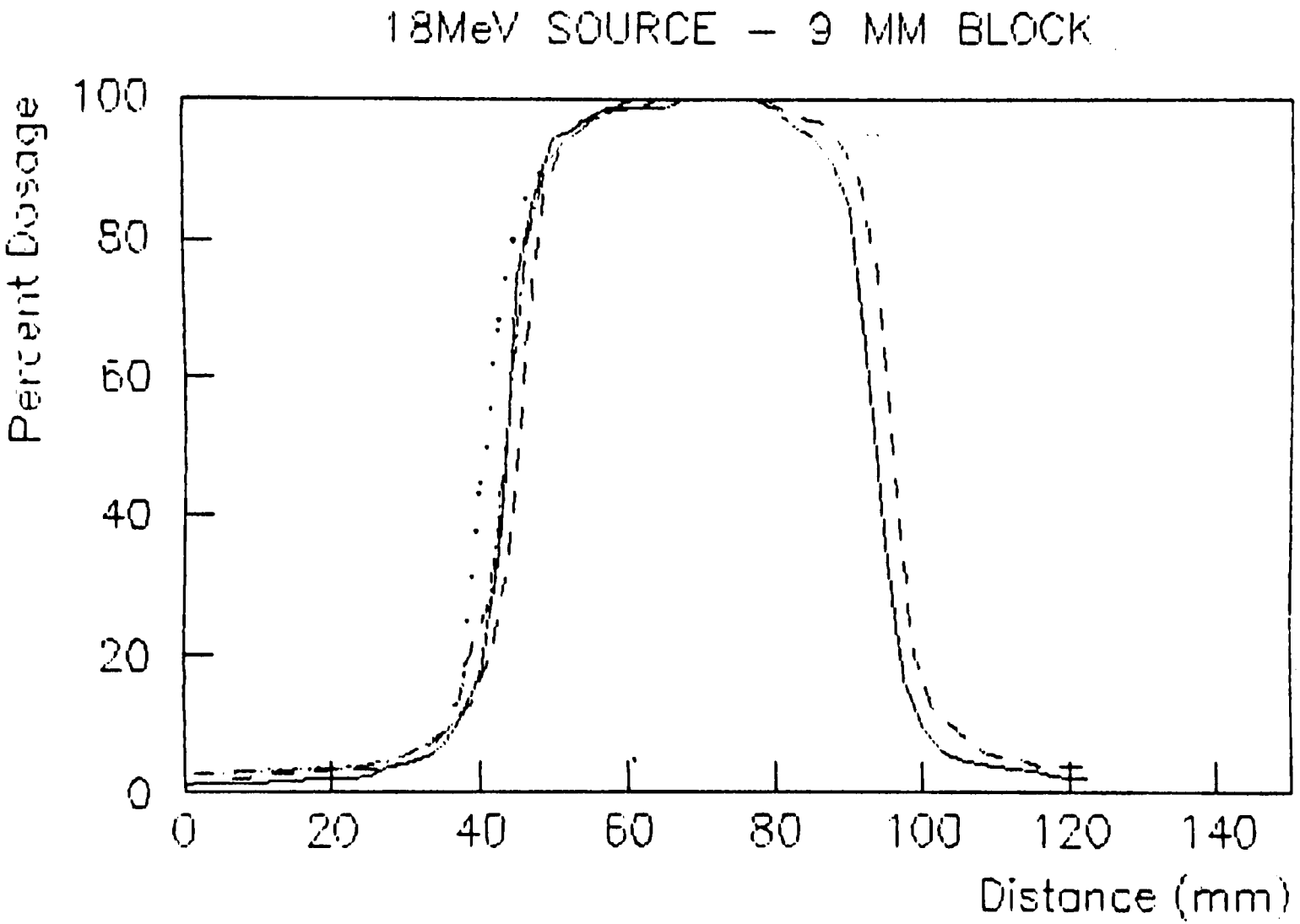

STRAIGHT EDGE
SCAN TYPE #1
SCAN TYPE #2
SCAN TYPE #3

Fig.14

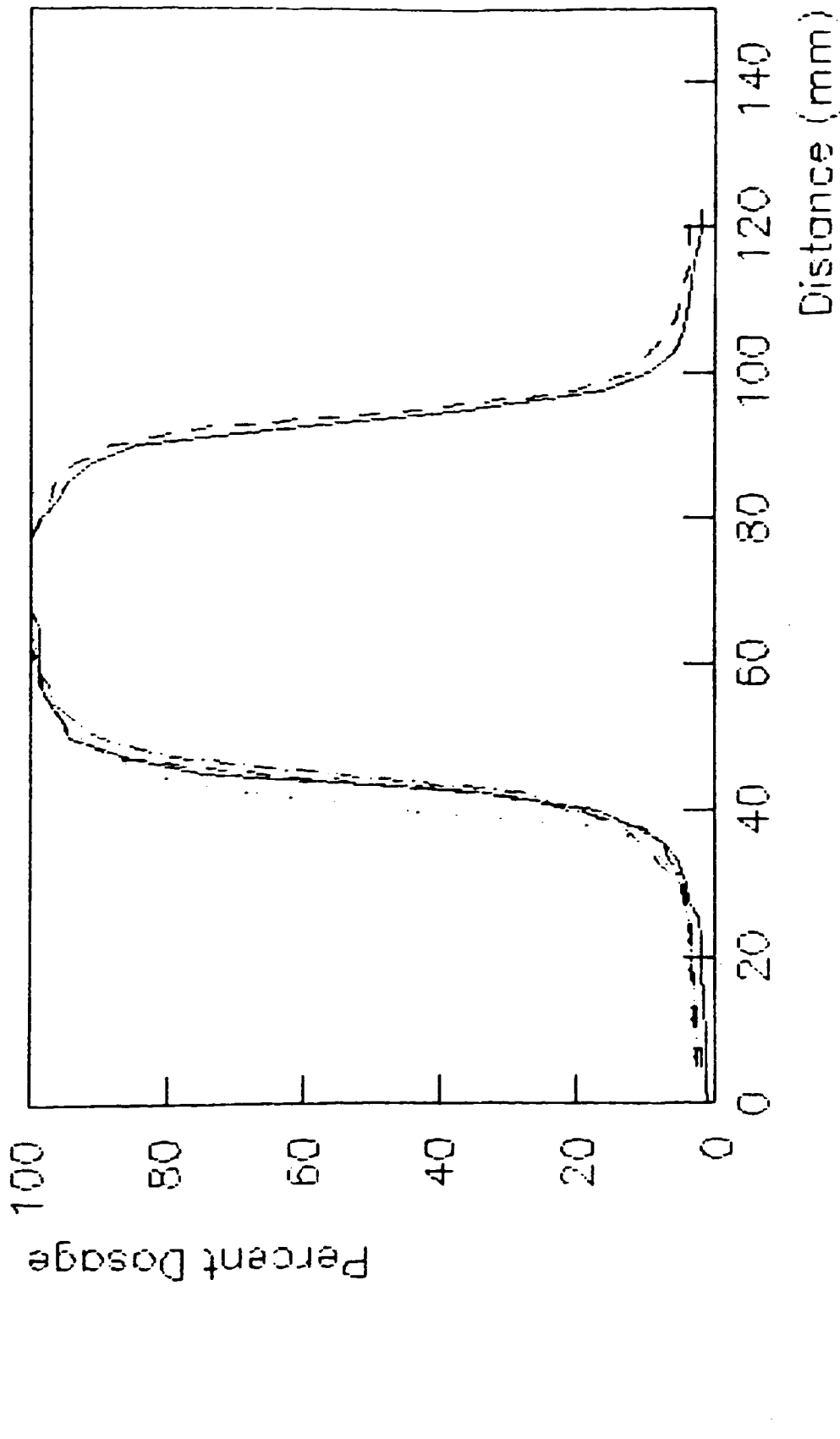
18 MeV SOURCE - 9 MM BLOCK
Percent Dosage
100
80
60
40
20
0
0
20
40
60
80
100
120
140
Distance (mm)
STRAIGHT EDGE
SCAN TYPE #1
SCAN TYPE #2
SCAN TYPE #3

Fig.15

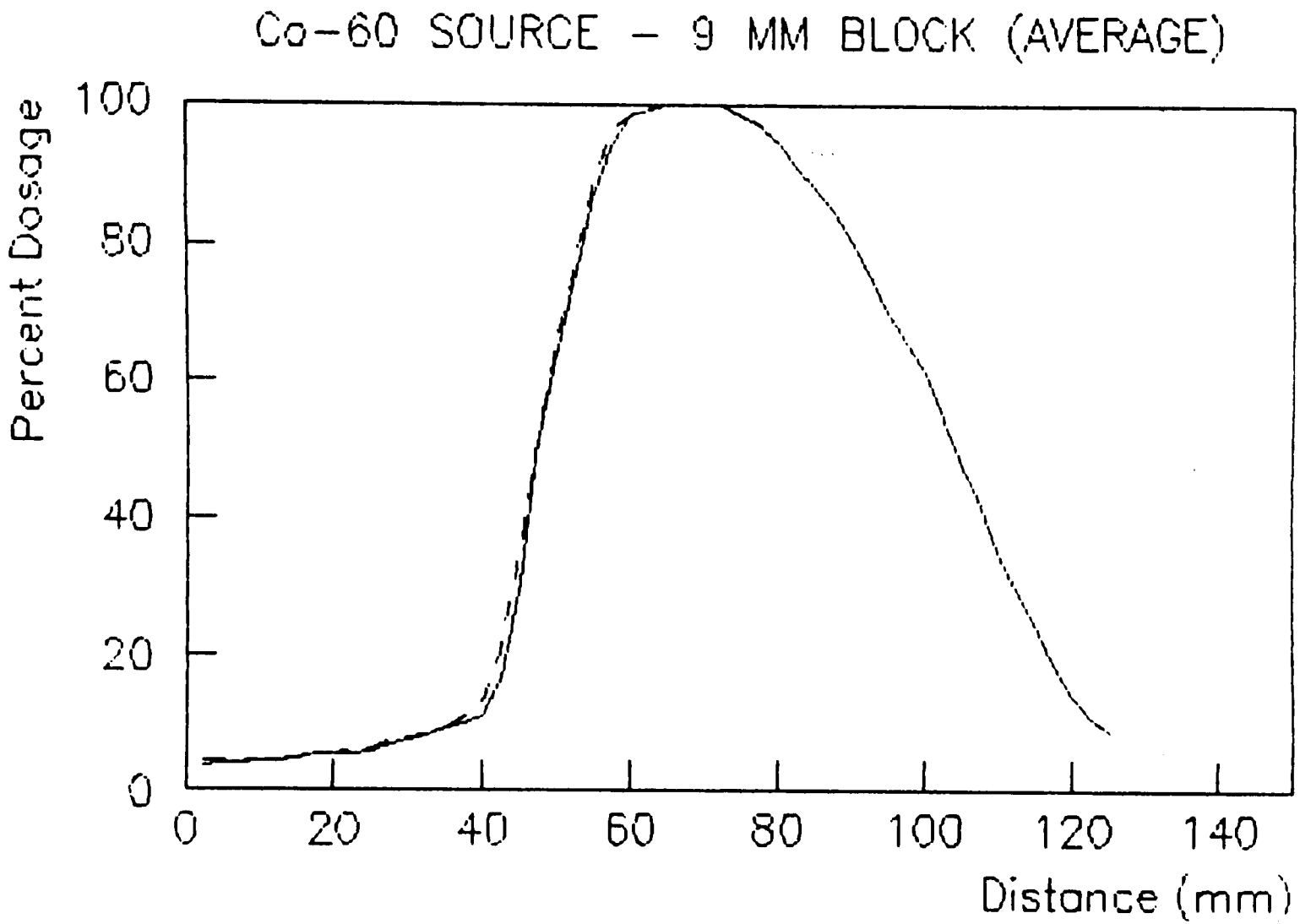

STRAIGHT EDGE

Fig.16

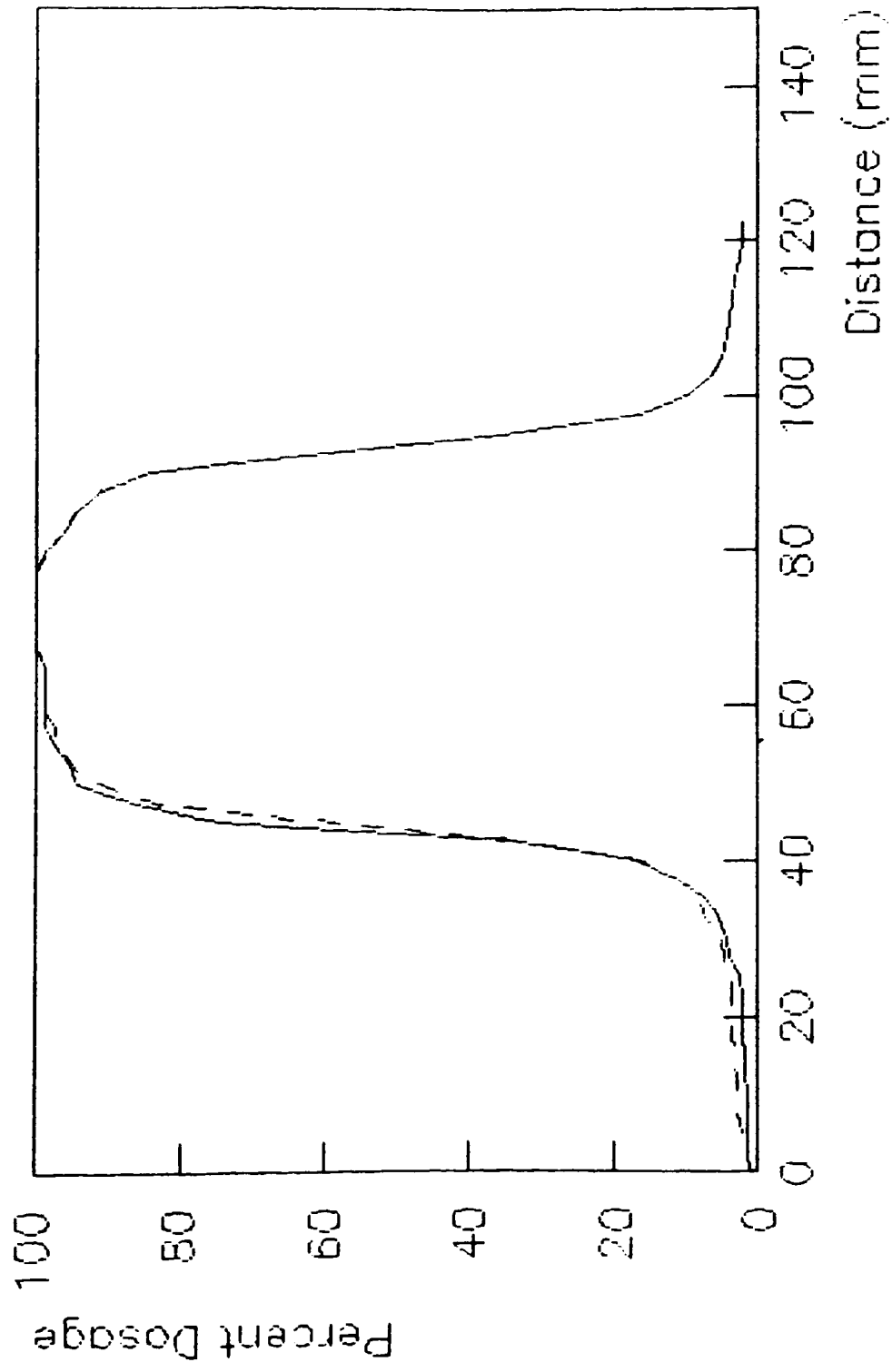
18 MeV SOURCE - 9 MM BLOCK (AVERAGE)
Percent Dosage
100
80
60
40
20
0
0
20
40
60
80
100
120
140
Distance (mm)
STRAIGHT EDGE

Fig.17

DISCUSSION

> When a patient is placed in a photon beam of known quality and quantity, the photons will be absorbed and scattered and both the quality and quantity of the beam will be changed. To study these changes, experiments have been performed using phantoms to replace the patient. The phantom should be of a material that will absorb and scatter in the same manner as tissue. Water and wet tissue absorb photons in the same way, and for this reason water has been used in many investigations. [15]

To simulate clinical conditions the exposures of the lead blocks were done in a water equivalent phantom at a depth of 10 cm. The depth of 10 cm was chosen because it is the average treatment depth, or half of the patient width.

In order to spare as much surrounding, healthy tissue as possible, treatments should be placed far enough apart to allow any healthy cells exposed to radiation enough time to repair themselves. But, spacing the treatments too far apart will allow the cancer to continue to grow. The latter consideration is given priority. Typically, radiotherapy sessions are administered five times a week for six weeks; totalling thirty sessions.

Verification films are made during treatments, under the radiation source, and are used to verify spatially where the dosage was absorbed. These films are difficult to evaluate and subject to the reader's interpretation. The ideal technological form of verification would be to image the receptor tissue relative to some fixed point outside the patient; which is impossible.

Owing to the lack of concrete verification, and the fact that a patient is never exactly in the same place relative to the source and the blocking device over N treatments, there is a random sampling process taking place. The probability distribution of this situation is assumed to be described by a gaussian.

Absorbed dose can at best be described by a confidence interval. Therefore, for each of the N treatments it can be said with a certain degree of confidence that the spatial effect of the blocking mechanism will lie within an interval centered around the average blocking effect.

Mean deviation defined as the product of the standard deviation and the square root of pi divided by two, is a term that is familiar to the physicians at the University of Rochester Cancer Center. Clinically, this describes the uncertainty in the position of the shielding block relative to the prescribed treatment

area in the patient. A mean deviation in the range of 4 to 12 mm. is common in radiotherapy.(See Appendix B)

The exposures of the block models represent the ideal situation of the block-patient orientation, in that there is no patient movement and only one exposure. The effect of movement in the patient, and variations in patient block orientations over N treatments would cause the block definition to become less destinct. Therefore, the results of scan types 1, 2, and 3 (See figure 5), were averaged to show a more realistic effect of the block edges over a series of treatments. This averaging process takes into account the effect of the stepped edge configuration over one period. All of the results are shown in reference to the penumbra obtained with the straight edge block.

The microdensitometer scans of the film samples were made perpendicular to the straight edge. The discontinuous edge film samples were scanned in three different specified positions (See Appendix A). These were made perpendicular to the theoretical straight edge that it is being contrasted to. A reference line was made on these samples to align the edge scan data spatially. The reference line was made perpendicular to the plane adjoining the peaks.

During the straight edge scan and scan type 1 on the microdensitometer, the scanning was continued past the normal field edge penumbra. In all cases, the open field edge had a greater spread function than any of the blocks. This is to be expected due to the blocks being closer to the receptor.

The spread function of the two sources varied widely; which can be seen from the results. This phenomenon can be attributed to the variation in source sizes. The Therac 20 (18 MeV), had a source size of 0.3 cm., nearly seven times smaller than the Co-60 (Picker Corp. CB-80) source. The wider the spread function, the more smoothing that occurs, thus a greater loss of detail information. This is the reason that the 6 and 9 mm block sizes are nearly indistinguishable from the straight edge for all scan types. Again, the spreading occurring for all of the scan types for the stepped edges is still much less than the field edge penumbra.

In the exposures made under the Therac, the detail of the block is much more evident due to its finer spread function of the system. This variation is shown on the percent dosage vs distance graphs for the Therac (See Results). Although the jaggard edges of the 18 MeV exposures have a more pronounced effect than the Co-60 exposures, the averaged effect of these blocks is similar to a straight edge.

CONCLUSION

The author's conclusion is based on an averaged block penumbral effect over N radiation treatments. This average penumbra being an averaged effect of one period of the jaggard edge. It can be concluded from the data that the average effect is more clinically realistic.

The data from the 9mm block exposures under the 18 Mev source, (unaveraged), have a spread between scan type one and scan type three, in the order of three millimeters. This is a spread that is well within the range of the interval defined by the 95% and 99% confidence interval limits, for average clinical mean deviation values (See Appendix B). This spread of three millimeters represents an exposure with no patient movement and only one sample rather than the average effect of N treatments. The data shows the average penumbra is less than or equivalent to the field edge penumbra thus supporting the hypothesis of the feasibility of a digitally-controlled bloxel, (block element) system.

Therefore, in conclusion, a digitally-controlled bloxel system would in the long run be cost efficient, quick, reproducible, and most importantly, and encourage physicians to block healthy tissue that

perhaps would have been overlooked. The exact size that would be operationally optimal should be investigated further by physicists, physicians, and mechanical engineers.

REFERENCES

1. Huang, D., et al., "Evaluation of Lead Acrylic as a Filter for Contaminant Electrons in Megavoltage Photon Beams," Med Phys, pp.93-95, 10(1), (1983).

2. Aldrich, John E., et al., "The Design of Shielding Windows using Lead Glass, Lead Acrylic, and Plate Glass," Rad, p.247, 146(1983).

3. Gray, Joel E., et al., "Shaped, Lead-Loaded Acrylic Filter for Patient Exposure Reduction and Image-Quality Improvement," pp.825-828, Rad, 146(1983).

4. Baily, B., et al., "A New Technique for the Radiation Shielding in Superficial X-ray Therapy," Bri J Rad, pp. 805-812, 54(1981).

5. Williamson, Jeffrey F., et al., "Film Dosimetry of Megavoltage Photon Beams: A Practical Method of Isodensity-to-Isodose Curve Conversion," Med Phys, pp.94-98, 8(1), (1981).

6. Walz, B. J., et al., "Individualized Compensating Filters and Dose Optimization in Pelvic Irradiation," Rad, pp.611-614, 107(1973).

7. Purdy, J.A., "Secondary Field Shaping," in Advances in Radiation Treatment Planning, Ed. Wright, A. E. and Boyer, A.L., (Hammond: Med Phys Monograph No. 9, 1982), pp. 456-476.

8. Powers, W. E., "A New System of Field Shaping for External-Beam Radiation Therapy," Rad, pp. 407-411, 108(1973).

9. Fraass, B. A., et al., "Clinical use of a Match-Line Wedge for Adjacent Megavoltage Radiation Field Matching," Int J Radiat Oncol Biol Phys, pp. 209-216, 9(2), (1983).

10. Morrison, Richard A., "Spherical Lead Shields for Megavoltage Teletherapy," Rad, pp. 546-547, 127(1976).

11. Simpson, L., U. R. Cancer Center, Oct. 20, 1983, personal correspondence.

12. ibid., May 1983.

13. ibid., Oct. 20, 1983.

14. ibid., Oct. 20, 1983.

15. Johns, H. E. and Cunningham, J. R., The Physics of Radiology, Charles C. Thomas, Springfield, p.370, p.337, (1983).

16. Swets, J. A., "ROC Analysis Applied to the Evaluation of Medical Imaging Techniques," Investigative Radiology, pp. 109-121, 14(1979).

17. Hanley, J. A., "A Method of Comparing the Areas under Receiver Operating Characteristic Curves Derived from the Same Cases," Rad, pp. 839-843, 148(1983).

18. Thijssen, M. A. O., "Receiver Operating Characteristic Curves in Diagnostic Imaging," Diagnostic Imaging, pp. 163-168, 52(1983).

19. Hammoudah, M. M. H., "Influence of Collimator Design on the Shape of Isodose Curves in High Energy Electron Beams," Journal of Medicine, pp.467-478, 10(6), (1979).

20. Davis, A., et al., "A Personal Dosimeter for Biologically Effective Solar UV-B Radiation," Photochemistry and Photobiology, pp.283-286, 34(1981).

21. Swensson, R. G., et al., "Omissions in Radiology: Faulty Search or Stringent Reporting Criteria?," Rad, pp.563-567, 123(1977).

22. de Vos, R. J., "An Accurate and Automatic Positioning System for Penumbra Wedges Applicable to the Radiotherapy of Hodgkin's Disease," Bri J Rad, pp. 339-340, 56(1983).

23. Metz, C. E., "Evaluation of Receiver Operating Characteristic Curve Data in Terms of Information of Theory, with Applications in Radiography," Rad, pp. 297-303, 109(1973).

24. Starr, S. J., et al., "Visual Detection and Localization of Radiographic Images," Rad, pp. 533-538, 116(1975).

25. Hanley, J. A., et al., "The Meaning and Use of the Area under a Receiver Operating Characteristic (ROC) Curve," Rad, pp.29-36, 143(1982).

26. Metz, C. E., "Observer Performance in Detecting Multiple Radiographic Signals," Rad, pp.337-347, 121(1976).

27. Lusted, L, B., "General Problems in Medical Decision Making with Comments on ROC Analysis," Seminars in Nuclear Medicine, pp. 299-306, 13(4), (1978).

28. Metz, C. E., "Basic Principles of ROC Analysis," Seminars in Nuclear Medicine, pp.283-298, 13(4), (1978). , pp. 283-298.

29. Goodenough, D. J., et al., "Radiographic Applications of Receiver Operating Characteristic (ROC) Curves," Rad, pp. 89-95, 110(1974).

30. Hogstrom. K. R., et al., "Electron Beam Dose Calculations," Phys Med Biol, pp. 445-459, 26(3), (1980).

31. Tesch, K., "Comments on the Transverse Shielding of Proton Accelerators," Health Physics, pp.79-82, 44(1), (1983).

32. Thatcher, M., "A Simple Equivalent Tissue-Air Ratio Method for Calculating Absorbed Dose in a Heterogeneous Medium," Rad, pp.527-529, 146(1983).

33. Yamaguchi, C., et al., "Effect of Tungsten Absorption Edge Filter on Diagnostic X-ray Spectra, Image Quality, and Absorbed Dose to the Patient," Phys

Med Biol, pp.223-232, 28(3).

34. Goodenough, D. J., et al., "Measurement of Observer Performance," , Quality Control in Nuclear Medicine, C. V. Mosby Co., Saint Louis, pp.118-127, (1977).

35. Moores, B. M., et al., "A Quantitative Evaluation of Film and Film/Screen Combinations for Mammographic Examination," Bri J Rad, pp.626-633, 52(1979).

36. Foley, W. D., et al., "The Effect of Varying Spatial Resolution on the Detectability of Diffuse Pulmonary Nodules," Rad, pp. 25-31, 141(1981).

37. Gehringer P., et al., "The (Gamma)- Response of Blue Cellophane Films under Controlled Humidity Conditions," Int J Appl Radiat Isot, pp.27-32, 33(1982).

38. Kepka, A. G., et al., "A Solid-State Video Film Dosimetry System," Phys Med Biol, pp.421-426, 28(4), (1983).

39. Braestrup, C. B., et al., "Shielding Design Levels for Radiology Departments," Rad, pp.445-447, 107(1973).

40. Kelsey, C. A., et al., "Anticrossover Emulsions Evaluated by Observer Performance Tests," Rad, pp. 209-211, 146(1983).

APPENDIX A

Co-60 Calibration Curve:

- Co-60 source calibrated at 29.66 rad/min on January 13, 1984 at 80 cm.,

(source used 59 days later).

- Co-60 half life = 5.271 years.

- Decay factor:

exp((-ln 2 / 5.271) x (59 / 365)) = 0.9797

- Tissue to air ratio (at a depth of 0.5 cm.) = 1.035

- Exposed at 124.5 cm.

Dosage:

(.9797)(29.66)(1.035)((80/124.5)^ 2) = 12.4 rad/min

Therac 20 (18 MeV) Calibration Curve:

- 100 Monitor units/minute

- 1 Monitor unit = 1 Rad (approximately) at Dmax = 3.5 cm.

- Tray transmission = 0.97

- Dose at 100 cm. = 100 rad (source calibration)

- Tissue to air ratio at a depth of 5 cm. for a 10 x 10 cm field = .997

Dosage:

(0.997 x 0.97 x 100 (rad/min)) / ((100 / 124.5)^2) = 149.9 rad / min

Block Exposures with Co-60 Source

- 80 days after calibration of source at 29.66 rad/min at 80 cm. from source.

- Decay factor:

exp((-ln 2 / 5.271) x (80 / 100)) = 0.97

- Tissue to air ratio at depth = 10 cm. for a 10 x 10 cm. field 100 cm. from source = .709

- Source to block distance = 64.5 cm.

- Source to film distance = 100 cm.

Dosage:

(0.97)(.709)((80 / 100)^2)(29.66 rad/min) = 13.1 rad/min

Block Exposures with Therac 20 (18 Mev)

- Tissue to air ration at depth = 10 cm., for a 10 x 10 cm. field at 100 cm. from source = .894

- 100 Monitor units/minute

- Transmission of tray = .97

Dosage:

dose = 100 (rad/min) / ((0.97)(0.894) = 115 rad/min.

Microdensitometer Scans

- Eyepiece = 5X

- Objective lens = 5X

- Aperture = 1.5 mm diameter

- Scan rate = 10 mm/min.

- Chart speed = 50.6 mm/min.

- Scan specification

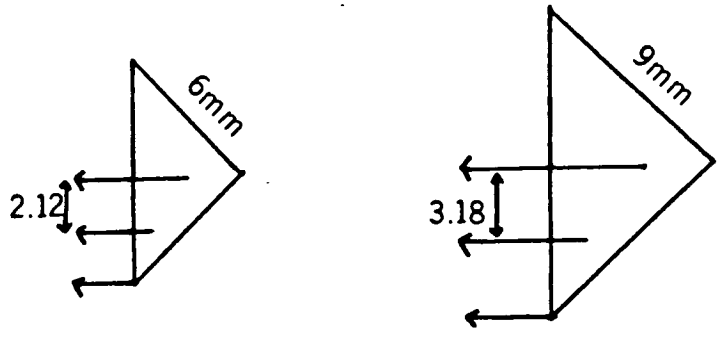

scan separation

Fig.19

APPENDIX B

Table 1 - 95% and 99% Confidence Interval (Sample size = 30)

mean deviation = 4 mm.

standard deviation = 5.01

95% Confidence Interval : $-1.79 < \bar{x} < 1.79$

99% Confidence Interval : $-2.33 < \bar{x} < 2.33$

mean deviation = 8 mm.

standard deviation = 10.02

95% Confidence Interval: $-3.58 < \bar{x} < 3.58$

99% Confidence Interval: $-4.66 < \bar{x} < 4.66$

mean deviation = 12 mm.

standard deviation = 15.04

95% Confidence Interval: $-5.38 < \bar{x} < 5.38$

99% Confidence Interval: $-7.00 < \bar{x} < 7.00$

APPENDIX C

Calculations utilized for Table 1 (Appendix B):

Sample size = 30

$$Z = (X - \mu) / (N / \sqrt{S})$$

Where:

X = Sample Average
N = Sample Size
S = Sample Standard Deviation

and:

A = Mean Deviation
$A = S\sqrt{\pi / 2}$

Z(alpha = 0.05) = 1.96
Z(alpha = 0.01) = 2.55

Fig.20

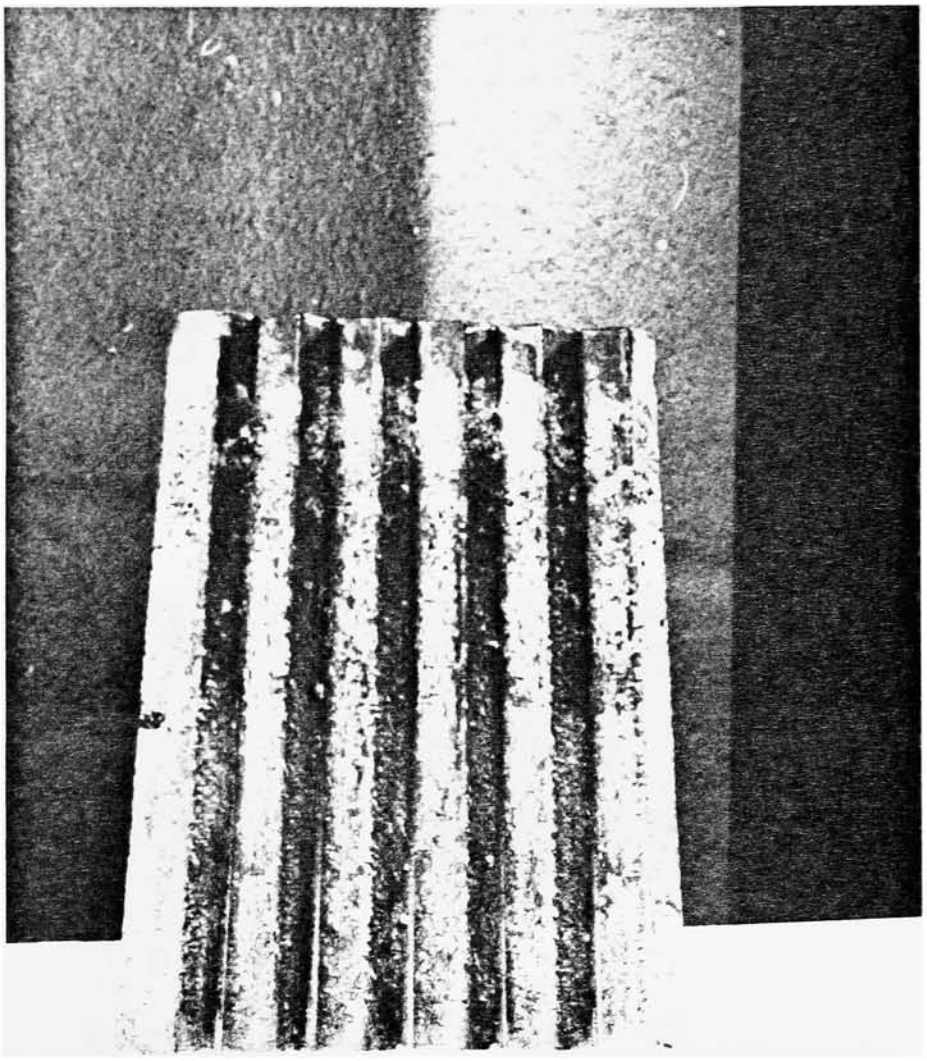

BLOCK
MODEL

X-RAYS

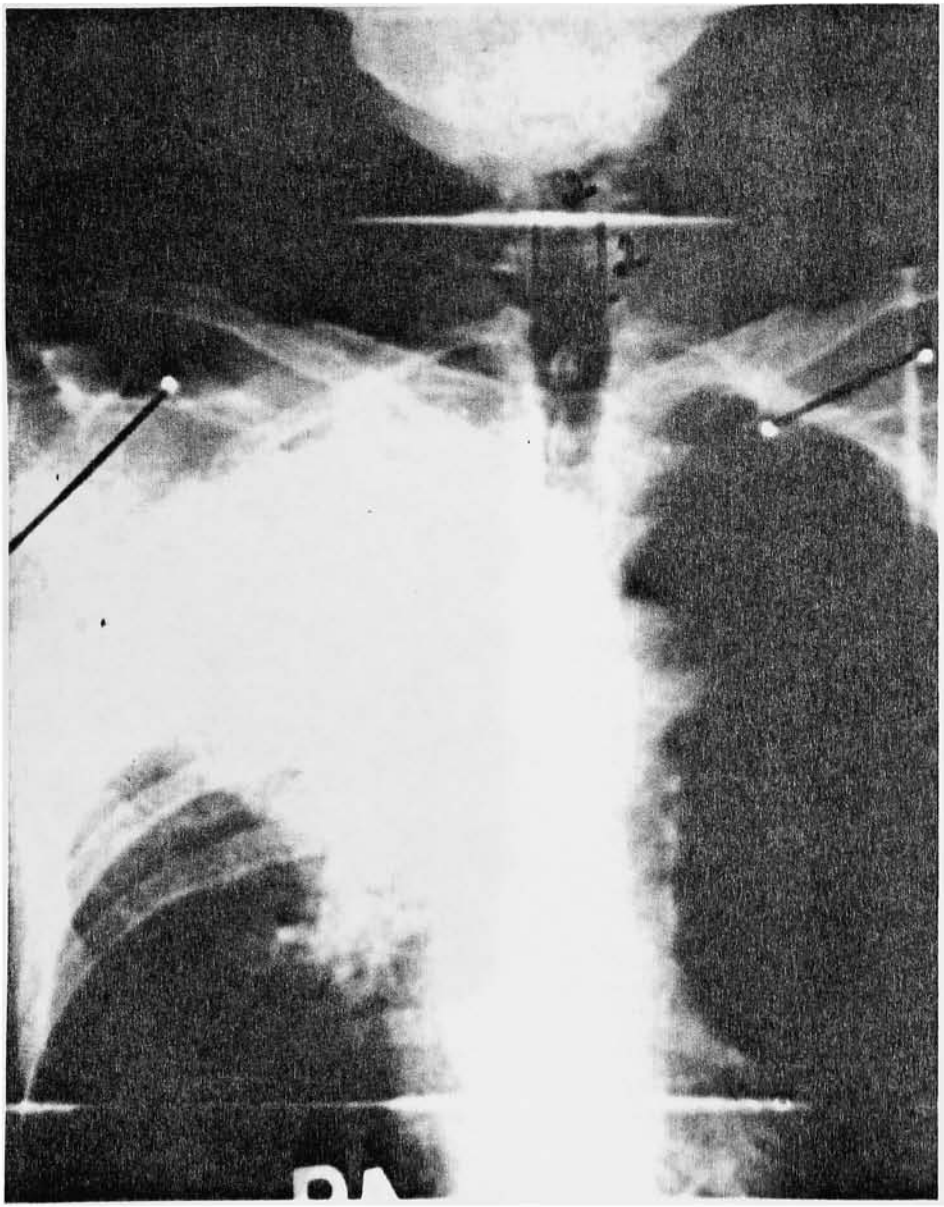

simulator

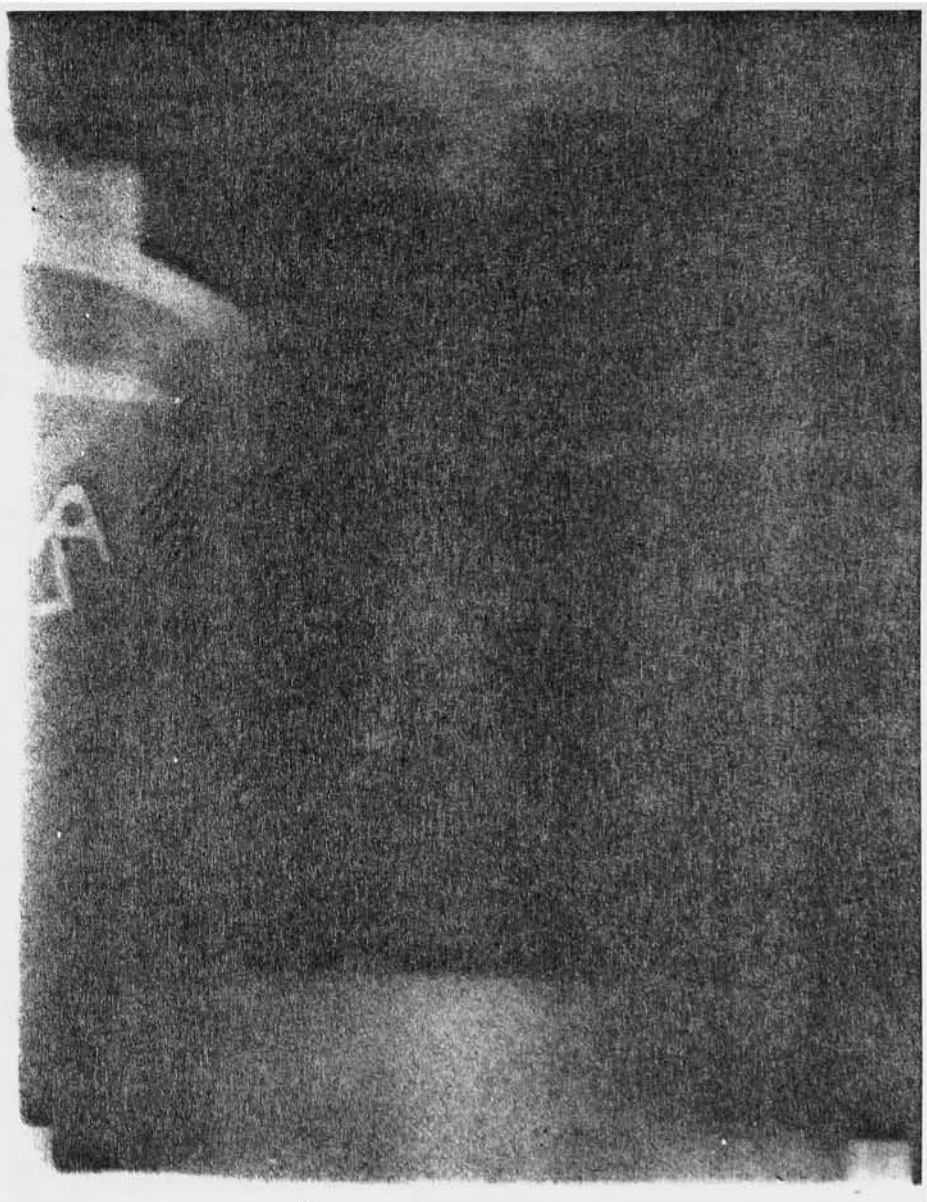

verification

Fig. 21

9 MM

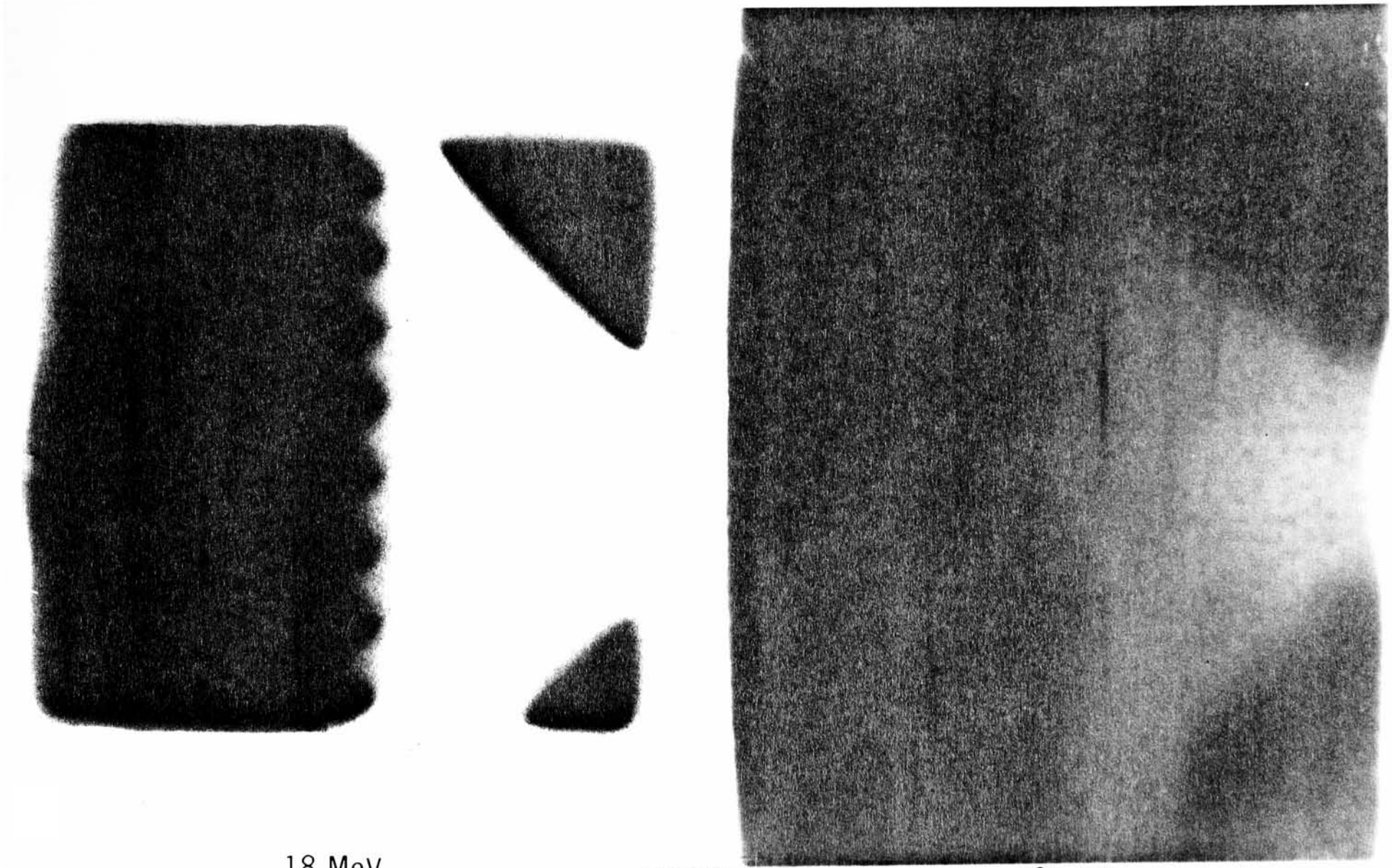

18 MeV

EXPOSURES

Co-60

Fig.22

VITA

The author was born in Portland Maine to John and Nancy Ciccone. Shortly thereafter moved to Maryland, where her father was stationed for military service. At the age of three, her family moved to Boston Massachusetts, where she grew up.

She attended the Revere public school system and in 1979 entered Merrimack College. In June of 1982 she transferred into the Imaging and Photographic Science program at Rochester Institute of Technology and received a bachelor of science degree in the Spring of 1984.

She looks forward to a challenging career in Imaging Science.